Carbohydrate Polymers 91 (2013) 22–32

Contents lists available at SciVerse ScienceDirect

Carbohydrate Polymers

journal homepage: www.elsevier.com/locate/carbpol

Bacterial exopolysaccharide based nanoparticles for sustained drug delivery, cancer chemotherapy and bioimaging

Sreejith Raveendran, Aby C. Poulose, Yasuhiko Yoshida, Toru Maekawa, D. Sakthi Kumar*

Bio-Nano Electronics Research Centre, Graduate School of Interdisciplinary New Science, Toyo University, Kawagoe, Saitama, 350-8585, Japan

ARTICLE INFO

Article history:
Received 8 May 2012
Received in revised form 11 July 2012
Accepted 30 July 2012
Available online 7 August 2012

Keywords:
Mauran
Sustained release
Bacterial polysaccharides
Extremophiles
Chitosan
Cancer therapy and bioimaging
Halomonas

ABSTRACT

Introduction of a novel biocompatible, stable, biomaterial for drug delivery application remains always challenging. In the present study, we report the synthesis of an extremophilic bacterial sulfated polysaccharide based nanoparticle as a stable biocompatible material for drug delivery, evaluation of anticancer efficacy and bioimaging. Mauran (MR), the sulfated exopolysaccharide extracted from a moderately halophilic bacterium, *Halomonas maura* was used for the synthesis of nanoparticles along with chitosan (CH). MR/CH nanoparticles were synthesized by simple polyelectrolyte complexation of anionic MR and cationic CH. The MR/CH hybrid nanoparticles formed were ranging between 30 and 200 nm in diameter with an overall positive zeta potential of 27.5 ± 5 mV and was found to be stable under storage in solution for at least 8 weeks. *In vitro* drug release studies showed a sustained and prolonged delivery of 5-fluorouracil (5FU) for 10–12 days from MR/CH nanoparticles under three different pHs of 4.5, 6.9 and 7.4 respectively. Cytotoxicity assay revealed that MR/CH nanoparticles were non-cytotoxic towards normal cells and toxic to cancer cells. Also, 5FU loaded MR/CH nanoparticles were found more effective than free 5FU in its sustained and controlled manner of killing breast adenocarcinoma cells. Fluorescein isothiocyanate (FITC) labeled MR/CH nanoparticles were used for cell binding and uptake studies; thereby demonstrating the application of dye tagged MR/CH nanoparticles for safe and nontoxic mode of live cellular imaging. We report the introduction of an extremophilic bacterial polysaccharide, MR, for the first time as a novel biocompatible and stable biomaterial to the world of nanotechnology, pharmaceutics and biomedical technology.

1. Introduction

Sulfated polysaccharides (SPSs) are gaining attention since last few decades because of their exceptionally best physico-chemical properties and bioactivities. Owing to their unique properties like stable structure, composition, fluid dynamics, extreme stability, biodegradability and biocompatibility, they are widely exploited in modern biotechnology and material science (Arad & Levy-Ontman, 2010; Xu, Zhang, Nichols, Shi, & Wen, 2007). Naturally occurring plant (algal) and animal sulfated polysaccharides are of great therapeutic importance apart from their food and industrial applications. They are proved to be effective in retroviral inhibition and cancer therapy. Most of the mammalian cell receptors that help in the adhesion of various growth factors during angiogenic processes (Cheng, Huang, Lur, Kuo, & Lu, 2009) and interacting with viral glycoproteins are SPS (Luscher-Mattil, 2000). Despite of their varying structure and composition, most of them are widely studied for their antiviral, anti-inflammatory, antitumor, anti-parasitic and anti-angiogenic activities as well as activation of immune system and effect of smooth muscle proliferation (Toshihiko, Amornrut, & Robert, 2003). These polymeric carbohydrate structures form important constituents of plants, animals and micro-organisms either as structural component or as storage molecules. Among various SPS, algal and animal polysaccharides were extensively studied; whereas bacterial polysaccharides are thus far been overlooked. Most of the SPS are polyanionic in nature and can bind to positively charged molecules *via* polyelectrolyte complexation or ionotrophic gelation. Hence they are widely used for nanotechnology applications including the synthesis of nanoparticles and microspheres for drug delivery purposes (Argandona et al., 2005; Bouchotroch, Quesada, Moral, Llamas, & Bejar, 2001; Calvo, Martinez-checa, Mota, Bejar, & Quesada, 1998; Quesada et al., 1990).

Extreme environments are proved to be interesting as a valuable source for industrially important bacteria that produces enumerable active biomolecules like polysaccharides, proteins and small peptides. Focus on active microbial sulfated exopolysaccharides (EPS) especially from extremophilic bacteria is of prime concern in current research for an ideal formulation of nanodrug carrier to encapsulate an anticancer test drug and demonstrate its sustained release pattern as well as anticancer efficacy. Halophiles are such extremophilic bacterial species that are seen under high

* Corresponding author. Tel.: +81 49 239 1375; fax: +81 49 234 2502.
E-mail address: sakthi@toyo.jp (D.S. Kumar).

0144-8617/$ – see front matter © 2012 Elsevier Ltd. All rights reserved.
http://dx.doi.org/10.1016/j.carbpol.2012.07.079

salt conditions of about 5–25% of NaCl. *Halomonas maura* is a moderately halophilic bacterium, which is capable of producing highly sulfated EPS residues into the external milieu. As reported by Arias et al. (2003), *Halomonas* polysaccharides are rich in sulfate residues and hence posses various biological properties. Polysaccharides of extremophilic bacterial origin have remarkably excellent properties that show their better future in the field of nanodrug drug delivery. Biologically active sulfated polysaccharide produced by *H. maura* is called MR and it has exceptionally high sulfate content and uronic acid content.

MR is a high molecular weight acidic polysaccharide with repeating units of mannose, galactose, glucose and glucuronic acid. It is highly anionic in nature due to the presence of sulfate and uronic acid moieties. Viscoelasticity, pseudoplasticity and thixotropic behavior of MR make it an ideal molecule for material science applications. Similarly rheological properties of MR are not easily affected by the presence of any salts, sugars, surfactants, lactic acid, and changes in pH and freeze thawing (Llamas et al., 2006). Another important striking property of MR is the ability to with stand various harsh conditions like temperature, freeze thawing, extreme pH values and salt conditions. High temperature over 55 °C has detrimental effect on viscosity, although it can regain its 70% of its property on cooling to 25 °C (Arias et al., 2003). MR can form stable gels on binding to various metal ions that helps in efficient removal of toxic ions from the polluted environments and water. The unusually high sulfate content of MR contributes to immunomodulating and antiproliferative effects on human cancer cells (Llamas et al., 2006).

Present study involves the extraction of MR from *H. maura* for the synthesis of nanoparticles along with CH, to encapsulate anticancer drug 5FU and labeling of free nanoparticles with a fluorescent moiety facilitating cell binding and uptake studies. CH is a widely used polysaccharide, produced by the deacetylation of chitin, a long chain polymer seen in the exoskeleton of crustaceans and cell walls of fungi. Basically CH is a linear polysaccharide with β(1–4) linked D-glucosamine and N-acetyl D-glucosamine residues with variable deacetylation percentage. It is rich in positively charged amino functional group and can easily undergo coacervation or ionic gelation with anionic polymers, macromolecules and polyanions upon contact in an aqueous medium (Grenha et al., 2010; Lin et al., 2009; Liu, Jiao, Liu, & Zhang, 2007). Drug loaded MR/CH nanoparticles are formed during polyelectrolyte complexation of 5FU-entrapped MR with CH under constant stirring. 5FU is a broad-spectrum antitumor drug that interferes with the DNA synthesis and inhibits the action of thymidylate synthase in solid tumors. However, serious side effects limit its wide application in the medical field. With an aim of reducing side effects and enhancing therapeutic index of 5FU many combinations of polymers are being tried so far (McCarron, Woolfson, & Keating, 2000; Sivabalan et al., 2011). Encapsulation of a hydrophilic drug within a biomaterial based nanoparticle will be less toxic and safer for biomedical applications. Also, sustained release of the drug for a prolonged period of time can enhance the efficacy of therapy and reduce patient compliance. Hereby, we report the synthesis of stable biocompatible nanoparticles using bacterial EPS, especially from an extremophilic origin, with multiple applications of drug delivery, cancer chemotherapy and bioimaging for the first time to best of our knowledge.

2. Materials and methods

2.1. Materials

CH and FITC was purchased from Tokyo Chemical Industry (TCI, Kasei), Japan. 5FU was procured from Nacalai Tesque Inc., Japan. Dulbecco's modified Eagle's medium (DMEM) and fetal bovine serum (FBS) from Sigma-Aldrich, USA and Gibco respectively. Alamar blue from Invitrogen, USA and all other chemicals used were of reagent grade.

2.2. Bacterial strain and mammalian cell lines

Moderate halophilic bacteria *H. maura* (ATCC 700995) was purchased and propagated as per the procedure mentioned in the product information sheet. On solid medium, the colonies were creamy, raised, glistening, circular and entire (Bouchotroch et al., 2001). Mouse connective tissue (L929) fibroblast cells and breast adenocarcinoma cells (MCF7) were procured from RIKEN Bioresource Centre, Japan.

2.3. Bacterial culture and MR production

The strain was grown in MY medium as mentioned elsewhere (Xu et al., 2007). Briefly, the growth medium composition: NaCl, 51.3 g; $MgCl_2{\cdot}6H_2O$, 9 g; $MgSO_4{\cdot}7H_2O$, 13 g; $CaCl_2{\cdot}2H_2O$, 0.2 g; KCl, 1.3 g; $NaHCO_3$, 0.05 g; NaBr, 0.15 g; $FeCl_3{\cdot}6H_2O$, traces; glucose, 10 g; yeast extract, 3 g; malt extract, 3 g; proteose peptone, 5 g; trace salt solution, 0.00325 g. Bacto agar (2 g/L) was added for the preparation of solid medium. Liquid medium was prepared, sterilized and inoculated with 1 ml of 48 h culture grown in the same medium (OD_{520} = 2.5) and incubated at 32 °C in a rotary shaker at 110 rpm for 15 days. Bacterial growth and EPS production were monitored in batch cultures of 500 ml Erlenmeyer flasks with 100 ml of medium in each. The experiment was performed in triplicates. At the end of incubation culture was centrifuged using an ultracentrifuge, Himac, CF12RX at 12,000 rpm for 1 h at 4 °C. Supernatant was precipitated out with cold ethanol and again centrifuged. Pellet was dissolved in ultra pure distilled water and purified using dialysis against distilled water (3–4 exchanges) for 48 h using Snakeskin pleated dialysis tubing from Thermo scientific of 10,000 MWCO. Purified MR was freeze dried and subjected to characterization. Total carbohydrates (Dubois, Gilles, Hamilton, Rebers, & Smith, 1956) and proteins (Smith et al., 1985) were estimated as described elsewhere.

2.4. Electron microscopy of the strain

Cells were taken from mid exponential phase culture of *H. maura* for electron micrographic study of the EPS layering the bacterial cell. Negative staining and ultra thin sectioning was performed as mentioned elsewhere with slight modifications in the protocol and viewed through transmission electron microscope (TEM) (JEOL, JEM-2200FS). *H. maura* bound to poly-L-lysine coated glass slides were chemically fixed as mentioned elsewhere (Bouchotroch et al., 2001) and sputter coated with Pt. Images were recorded using scanning electron microscope (SEM) (JEOL, JSM-7400F).

2.5. MR characterization

Partially purified MR was subjected to X-ray photoelectron spectroscopy (XPS) (KRATOS). Analysis was carried out under a basic pressure of 1.7×10^{-8} Torr and the X-ray source used was anode mono-Al with pass energy of 40 (survey scan). XPS spectra for MR with peaks of C, N, O, S, and P were obtained. Fourier transform infrared (FTIR) spectroscopy was performed to characterize the structure of sulfated polysaccharide, MR. 2–3 mg of MR powder was mixed with 200 mg of dry KBr pellets, ground thoroughly and mixture was pressed into a 16-mm-diameter mold to prepare pellets for FTIR analysis. Infrared spectra were recorded (Perkin Elmer US) with a resolution of 4 cm^{-1} in the region of 4000–400 cm^{-1}

(Nicholas et al., 2005; Rougeaux, Pichon, Kervarec, Raguenes, & Guezennec, 1996).

2.6. Nanoparticle formulation and characterization

2.6.1. Synthesis of MR/CH nanoparticles

MR/CH based hybrid nanoparticles were prepared by spontaneous complex formation between MR and CH under strong magnetic stirring. Using the method described by Santo, Duarte, Gomes, Mano, and Reis (2010) for nanosphere formulation for CH and a polyanionic molecule, MR based nanoparticles were prepared. Briefly, CH was dissolved in 1% (w/v) acetic acid to obtain 6 mg/ml final strength, while a series of MR concentrations were prepared in distilled water and obtained different solutions with 1–5 mg/ml concentrations. Suspensions of nanoparticles were formed spontaneously when CH solution was added to MR solution under strong magnetic stirring at room temperature. Individual concentrations of the MR were checked separately for the accumulation of nanoparticles on mixing with CH molecules. Nanoparticle suspensions were subjected to characterization studies using electron micrograph before and after the process of filtration.

2.6.2. Effect of pH

Effect of pH on nanoparticle formation was studied using various pH combinations of MR and CH solutions respectively. MR solutions with a pH range of 3–7 were prepared separately and mixed with CH solution of pH range 2–5 respectively and observed for nanoparticle formation. Optimal pH range of MR and CH solutions were found out for a stable nanoparticle formation.

2.6.3. Effect of MR/CH concentration

Effect of concentration of MR in the nanoparticle formation was studied by keeping the CH concentration stable. Two different concentrations, 6 mg/ml and 3 mg/ml of CH solution was prepared and subjected individually to polyelectrolyte complexation with MR solutions of concentrations ranging from 1 to 7 mg/ml and 1 to 3 mg/ml respectively. Both, the least concentration and optimal ratio of MR and CH required for the nanoparticle formation were found out.

2.6.4. Characterization of MR/CH nanoparticles

Morphological features of the MR/CH nanoparticles formed were characterized using TEM and SEM. One drop of nanoparticle suspension was placed on carbon coated copper grid after hydrophilizing the grid for 30 s in a TEM grid hydrophilizer (JEOL DATUM, HDT-400) and dried thoroughly. Nanoparticles were observed using TEM under 200 kV and images were recorded. Surface characteristics of the nanoparticles were analyzed using SEM. Samples were prepared on various substrates like silica, poly-L-lysine coated glass and Sn substrates. Vacuum dried samples on silica and poly-L-lysine coated glass were sputter coated with Pt on a high resolution sputter coater (Hitachi, E-1030, Ion sputter), where as sample on Sn substrate were directly viewed under SEM. Simultaneously, detection of various constituent elements was also performed using energy-dispersive X-ray spectroscopy (EDS). FTIR (Perkin Elmer US) spectrum was also recorded for MR/CH nanoparticles and compared with individual spectrum of both MR and CH respectively. Particle size and the zeta potential were measured using Zetasizer (Malvern, Nano-ZS).

2.7. Drug encapsulation and release kinetics

2.7.1. Drug encapsulation and analysis

Incorporation of test drug, 5FU was performed for studying the drug encapsulation efficiency and its release kinetics from the MR/CH nanoparticles. 5FU of 2.5 mg/ml concentration was prepared using methanol and mixed with the MR solution before nanoparticle fabrication. Drug containing MR solution was stirred thoroughly for approximately 30 min before ionotrophic gelation with CH. Later, CH solution was added drop wise to 5FU containing MR solution under strong magnetic stirring. Drug loaded nanoparticles formed were centrifuged at 12,000 rpm for 10 min and supernatant was decanted carefully. Then the pellets were weighed and resuspended in 18 Ω ultra pure water. 100 μl of the drug loaded samples were drawn before and after centrifugation step, to calculate the encapsulation efficiency and loss of the trapped drug during centrifugation. Concentration of 5FU was determined using reverse-phase HPLC (RP-HPLC) (Shimadzu SCL-10A-VP System controller, SPD-M10A-VP Diode array detector, SIL-10AD-VP Auto Injector, LC-10AD-VP Liquid chromatograph) comprising a GL Sciences Inc., 5 μm, Inertsil ODS-3, 4.6 × 250 mm analytical column (McCarron et al., 2000). Entrapment efficiency was calculated as the difference between the drug used for encapsulation and the free drug available in the supernatant (Nair, Jagadeeshan, Nair, & Kumar, 2011). Percentage of encapsulation efficiency was calculated using the following equation:

$$\%\ \text{of encapsulation} = \frac{C_i - C_f}{C_i} \times 100$$

where C_i is the initial drug concentration and C_f is the free drug concentration in the supernatant. UV–vis absorption spectra of MR, CH, free 5FU, MR/CH and 5FU-MR/CH nanoparticles were recorded using Beckman UV–Visible spectrophotometer (DU730, Beckman Coulter) for the confirmation of nanoparticle formation and 5FU encapsulation.

2.7.2. In vitro drug release kinetic studies

Diffusion of 5FU from MR/CH matrix was carried out using a thermostatically maintained *in vitro* setup. Two different nanoparticle suspensions (sample stored at 4 °C for 3 months and a freshly prepared sample) were studied at two different pH conditions of 6.9 and 7.4 respectively using 50 ml Phosphate buffer solution (PBS). 0.5 ml of 5FU loaded nanoparticle solutions were taken in separate dialysis cassettes (MWCO 10 kDa) to study the drug release kinetics. In addition, a sample stored at 4 °C for 3 months was used to study the release under an acidic pH of 4.5 using sodium phosphate buffer solution. All experiments were performed in triplicates. The setup was incubated at 37 °C under a continuous shaking of 100 rpm for 12 days. At predetermined intervals, 90 μl of samples were collected from the receptor medium and the amount of 5FU released was determined using Beckman UV–Visible spectrophotometer at 266 nm. An equal volume of fresh dissolution medium was replaced for maintaining the sink conditions. Amount of the drug released to the receptor phase was evaluated using a standard curve for 5FU. Also the cumulative concentration found in the dissolution medium was evaluated by RP-HPLC.

2.8. In vitro cytotoxicity and cell uptake studies

2.8.1. Cell culture

L929, mouse fibroblast cell line and MCF7, breast cancer cell lines were used for testing the *in vitro* cytotoxicity of MR/CH nanoparticles and 5FU loaded MR/CH nanoparticles respectively. L929 cells and MCF7 cells were cultured and maintained separately using DMEM, supplemented with 10% of FBS at 37 °C in a 5% CO_2 atmosphere. Cells were sub-cultured after attaining confluent growth and seeded into 96 well plates for testing cytotoxicity and 33 mm glass base dish for imaging in the order of 5000–8000 cells/well and 3×10^4–6×10^4 cells/plate, respectively.

2.8.2. Alamar blue assay

Alamar blue assay was performed to detect the percentage of cell viability on the basis of the natural reducing power of the healthy cells, to convert resazurin to a fluorescent molecule, resorufin. Quantification of the cell viability in the presence of 5FU loaded MR/CH nanoparticles will indirectly measure the cytotoxicity caused by these nanoparticles. Alamar blue assay was performed as per the standard protocol. L929 cells were grown in 96 well plates for 24 h and treated with varying concentrations of MR/CH nanoparticles (50, 100, 250, 500 and 1000 μg/ml) to check its biocompatibility toward normal cells. Anticancer activity of 5FU-MR/CH nanoparticles was tested using MCF7 with a comparison to free drug 5FU. 5FU-MR/CH nanoparticles and free drug 5FU were taken with five different concentrations (50, 100, 250, 500 and 1000 μg/ml) respectively. Five consecutive days' studies were performed with MCF7 cells to analyze the sustained release of 5FU from MR/CH nanoparticles and its effect on cell death. 10% of alamar blue dye was added to each of the plates and kept for 4 h after an incubation of 24, 48, 72, 96 and 120 h respectively. At the end of incubation, fluorescence was measured at 580–610 nm, using a multi detection microplate reader (Dainippon Sumitomo Pharma, Powerscan HT). Experiment was conducted in triplicates and percentage of cell viability was evaluated using statistical analysis by deducing the mean values and standard deviation.

2.8.3. Synthesis of fluorescent MR/CH nanoparticles

FITC was used to label CH before synthesizing MR/CH nanoparticles. FITC labeled CH was synthesized based on the reaction of the isothiocyanate group of FITC with the primary amino group of CH (Ge et al., 2006). 1 mg of FITC in 1 ml of dehydrated methanol was treated with 3 mg of CH in 1 ml of 1% acetic acid solution under strong magnetic stirring. After 3 h of reaction in dark at ambient temperature, FITC labeled CH was added to aqueous solution of MR (3 mg/ml), to form MR/CH-FITC *via* polyelectrolyte complexation. Nanoparticles were collected using ultracentrifugation after washing the pellets with ultra pure water and stored for cell uptake studies. UV–vis spectra for FITC, MR/CH and MR/CH-FITC were recorded and compared.

2.8.4. Cellular binding and uptake of MR/CH-FITC nanoparticles

As mentioned earlier, MCF7 cells were grown in 33 mm glass base dish in the order of 3×10^4–6×10^4 cells/plate and were treated with 300 μl of MR/CH-FITC nanoparticles with 1 mg/ml concentration. After the incubation for 24 h, medium was removed and

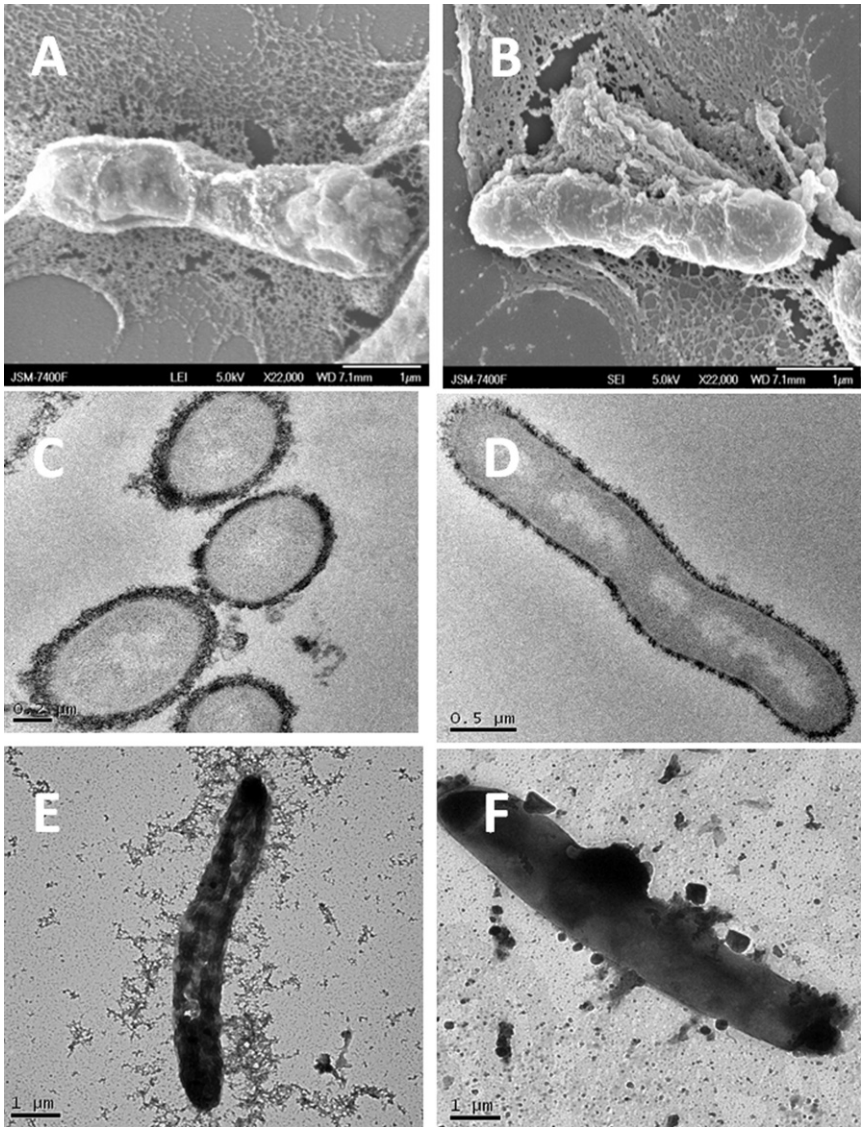

Fig. 1. SEM images of *Halomonas maura* showing MR accumulation (A, B); TEM images of ultra thin section of *Halomonas maura* showing MR accumulation (C, D); TEM images of negatively stained *Halomonas maura* showing MR accumulation (E, F).

the cells were washed with PBS and viewed under phase contrast-epifluorescence microscope (Nikon ECLIPSE, TE2000-U). Emission filter of 488 nm was used to observe the fluorescence emitted by MR/CH-FITC.

3. Results and discussion

3.1. Bacterial study and MR characterization

Electron microscopic studies of *H. maura* revealed the accumulation of MR on the cell wall of bacteria in the form of a granular sheath covering the entire bacterium. It was found that the cells during the mid exponential phase started releasing EPS to their external milieu, which was evident during the microscopic studies. Fig. 1A and B shows the SEM images of the ruthenium red stained bacterium from mid-exponential phase showing the release of MR from the cell wall. It was found that MR consists of nanosized globules joined together by a network of sticky fibrils. Fig. 1C shows the TEM image of the ultra thin sections of *H. maura* which is 2 days old, with varied amount of MR around the bacterium. It demonstrates the granular nature of the MR, which releases to the medium on maturation. Fig. 1D shows the TEM image of ultra thin section of 4 days old *H. maura* with comparatively lesser amount of MR surrounding the cell. Fig. 1E and F depicts the negatively stained image of *H. maura* showing MR accumulation and released globules around the cell respectively.

Partially purified MR after lyophilization was dry creamy-white in appearance. On chemical analysis using colorimetric reactions, it was found that the total carbohydrate concentration in MR extracted was $73 \pm 0.02\%$ and protein content was about $2.9 \pm 0.5\%$. As already reported by Arias et al. (2003), MR is an anionic SPS of average molecular weight of 4.7×10^6 Da with high uronic acid content. MR produced under optimal conditions posses glucose, mannose, galactose and galacturonic acid as four constituent sugar components. It also has a high sulfate content of 6.5% (w/w) that contributes to its polyanionic nature. Furthermore, MR also contains 1.3% of phosphate residues (Arias et al., 2003). The presence of S and P was confirmed by elemental analysis of MR using XPS. The peak showing at 168 eV depicts sulfate peak of MR. Fig. 2 a shows the characteristic ESCA peaks of elements in MR. Polysaccharide structure and the presence of sulfate moiety was estimated using FTIR spectra of MR in Fig. 2b. As common to all polysaccharides two characteristic peaks appeared at 3432 cm^{-1} and 2932 cm^{-1} assigned to O—H and C—H stretching vibrations respectively. Similarly, strong absorption bands at 1131 cm^{-1} and 1057 cm^{-1} may be assigned to C—O and C—C stretching in the pyranoid ring. In addition, the band at 979 cm^{-1} can be due to C—O—C stretching of glycosidic linkages. Two strong peaks at 1739 cm^{-1} and 1650 cm^{-1} can be assigned to carbonyl groups in two respective forms, carboxylic ester (C=O) form and carboxylate anionic (COO—) form. These carboxylic stretching vibrations can be from the uronic acid residues in MR. Spectral vibration at 1419 cm^{-1}

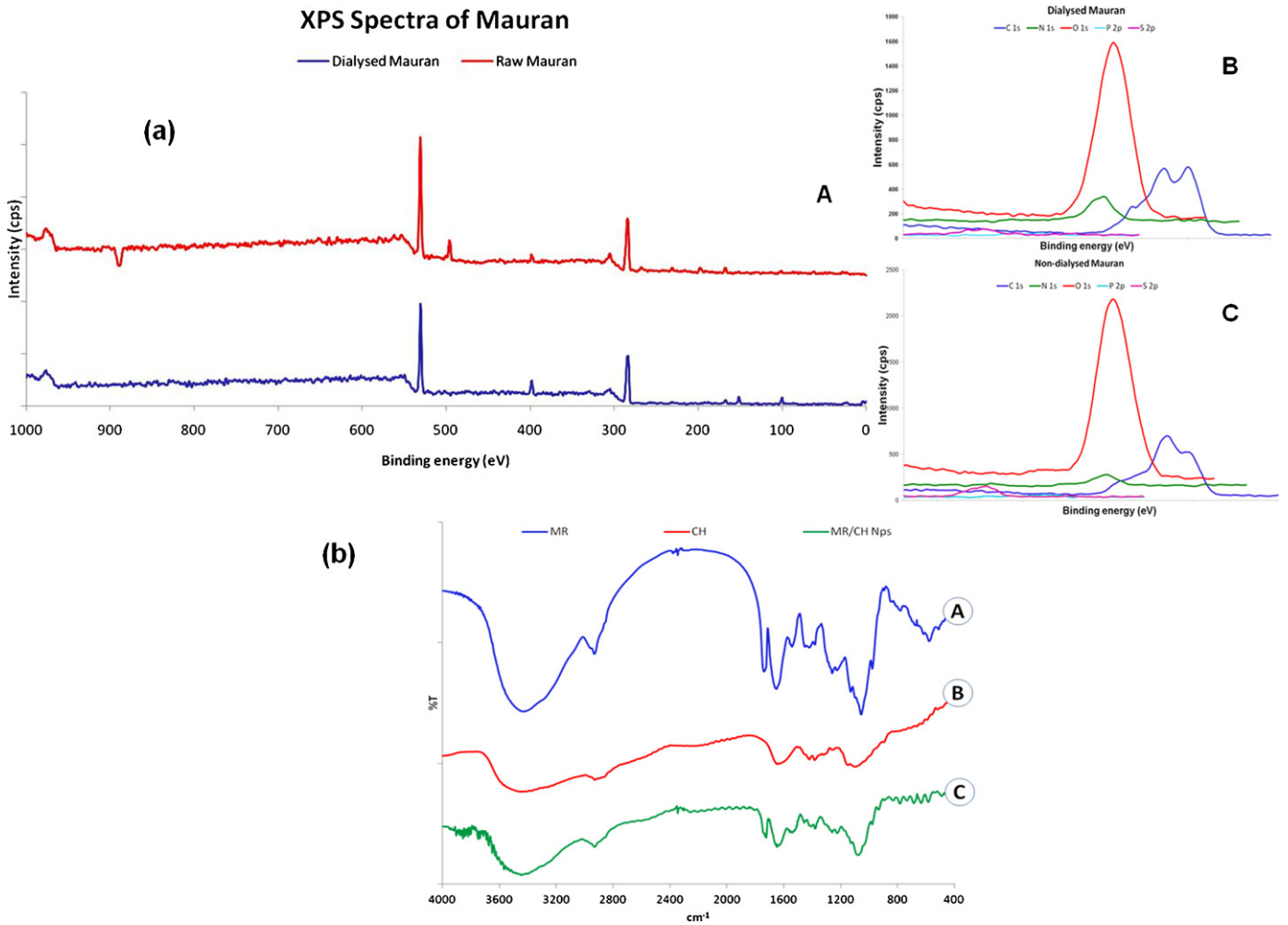

Fig. 2. (a) XPS spectra of raw and dialysed MR (A), intensity of elemental composition in raw MR (B), intensity of elemental composition in dialysed MR (C); (b) FTIR spectra of MR (A); CH (B); MR/CH nanoparticles (C).

Table 1
Combinations of various pH ranges of CH and MR in nanoparticle synthesis under optimal concentration.

pH of CH	pH of MR	Polyelectrolyte complexation
5	5.5	Precipitate
4	5	Precipitate
3.5	4	Precipitate
3	4.9	Aggregates
2.5	4.5	Nanoparticles formed
2.5	3.5	Nanoparticles formed

may be assigned to C—OH deformation vibration of carboxylate symmetric stretching. The sharp peak at 1261 cm^{-1} and its shoulder vibration at 1225 cm^{-1} confirms the presence of sulfate ester groups (S═O) which is a characteristic component of MR (Dev et al., 2010; Gomez-Ordonez & Ruperez, 2011). Comparison of MR with MR/CH nanoparticles and CH spectra will be discussed later in this section.

3.2. Nanoparticle formulation and characterization

CH molecule on poly-electrolyte complexation with anionic polysaccharides can spontaneously give rise to nanoparticles under strong magnetic stirring (Janes, Calvo, & Alonso, 2001). Various concentrations of MR were mixed with CH solution in 1% acetic acid separately under strong magnetic stirring to form nanoparticles of size ranging from 30 to 200 nm. pH as well as concentration of the CH and MR solutions plays a crucial role in the formation of nanoparticles and in its polydispersity. Different pH combinations were checked for the optimal level formation of stable nanoparticles. At pH 5 and higher, unstable macro clusters were formed. When the pH of CH solution was in the range 2.5–3, and MR solution in the range of 3.5–4.9, well isolated spherical nanoparticles were formed. Gradual increase in the pH value of MR solution to neutral resulted in large precipitate formation. Similarly on decreasing the pH values of both MR and CH solution acidic range, 3 or below resulted in precipitation. Nanoparticles prepared at an optimal acidic pH of 2.5–4.9 were found to be stable at least for 8 weeks. Various combinations of the pH values for CH and MR solutions separately used were depicted in Table 1. Effect of concentration of MR in nanoparticle formation was studied by keeping two different concentrations of CH stable. Combinations of various concentrations of CH and MR solutions separately used for nanoparticle formation are depicted in Table 2. When the concentration of CH was 6 mg/ml, and the MR concentration varied between 1 and 7 mg/ml, an increase in the size of the particles was observed. Large aggregates were formed when the ratio was 6:6 and on increasing ratio to 6:7, macro globules discernible to naked eyes were formed. While the nanoparticle suspension formed with a ratio of 6:5 was characterized to have poly-dispersed nanoparticles of range 30–150 nm approximately.

Table 2
Combinations of various concentrations of CH and MR in nanoparticle synthesis under optimal pH.

CH concentration (mg/ml)	MR concentration (mg/ml)	Polyelectrolyte complexation
6	1	No nanoparticles
6	2	No nanoparticles
6	3	Precipitate
6	5	30–150 nm particles
6	5.5	Nanoparticle aggregates
6	6	Nanoparticle aggregates
6	7	Macro globules
3	3	30–500 nm particles
3	2	30–500 nm particles
3	1	No nanoparticles

However, no particles were observed when the MR concentration was reduced below 3 mg/ml by keeping CH concentration at 6 mg/ml. In another experiment, the CH concentration was reduced to 3 mg/ml and MR concentration was altered from 1–3 mg/ml. It was observed that 3:2 was the least ratio required for nanoparticle formation where as 3:3 was the ratio required for stable and long lasting nanoparticle formation. The particles formed under later concentration were found to be stable for at least 8 weeks on SEM observation. Nanoparticles formed under optimal pH range of 2.5–4.9 at various ratios of 6:5 and 3:3 were found to have size ranging from 30 to 200 nm, with polydispersity index of 0.69 ± 0.03 and a positive zeta potential value of ζ 27.5 ± 5 mV. The overall positive charge of the MR/CH nanoparticles can be attributed to the higher concentration of CH molecules, which could favor the adsorption of negatively charged peptides or drug molecules during drug loading process. Positively charged nanoparticles can facilitate effective binding with negatively charged cell surfaces ensuring targeted drug delivery (Lin et al., 2009). Also free sulfate groups of MR/CH nanoparticles can compete with the binding mechanisms of various etiological agents with proteoglycan receptors during several disease conditions (Hosoyo, Balzarini, Shigeta, & Clercq, 1991; Liu, Jiao, Wang, Zhou, & Zhang, 2008). This will also facilitate the transport of drug across the cell membrane more quickly. Hence so obtained MR/CH nanoparticles can be ideal for drug delivery applications

Morphology of the nanoparticles formed was characterized by SEM and TEM. Fig. 3 shows SEM images of MR/CH nanoparticles adhered to the surface of various substrates. The surface morphology studied using SEM revealed that MR/CH nanoparticles formed were having spherical shape with smooth surfaces. Apart from spherical MR/CH nanoparticles various quasi-spherical and cubical particles were also observed (data not shown). Fig. 4 shows the TEM images of MR/CH nanoparticles in grape-like clusters. Interactions of various functional groups during nanoparticle formation were confirmed by FTIR spectroscopy as shown in Fig. 2b. Spectrum of MR/CH nanoparticles was compared with the individual spectrum of MR and CH. The peak at 1650 cm^{-1} in CH spectra indicates the presence of amide linkage ($CONH_2$) and in MR spectra indicates the carboxylate anion (COO—) form. This peak disappears and new peak at 1641 cm^{-1} appears with reduced intensity in MR/CH spectra. This can be due to the interaction of few amino groups of CH with carboxylate group of MR during ionic gelation. The peak at 1057 cm^{-1} in MR spectrum was weakened and shifted to 1078 cm^{-1}. Also the peak at 1739 cm^{-1} in MR spectra indicating carboxylic ester frequency in ring structure was shifted to 1727 cm^{-1}. Furthermore, the intensity of sulfate peaks at 1261 cm^{-1} and 1226 cm^{-1} was weakened in MR/CH spectra. This may be due to fewer interactions of free sulfate groups of MR during bond formation in MR/CH nanoparticles (Bhumkar & Pokharkar, 2006; Gomez-Ordonez & Ruperez, 2011; Huang, Sui, Wang, & Jiao, 2010). Similarly the interaction of amino and carboxylic groups and presence of sulfate groups in the nanoparticles formed were better explained by SEM-EDS image. Fig. 5 demonstrates the elemental mapping of MR/CH nanoparticles. Fig. 5A shows the corresponding reference image of EDS analysis of the MR/CH nanoparticles. Fig. 5B and C shows the density of C atoms and N atoms in the nanoparticles respectively. Also it confirms the interaction of carboxylic group of MR and amino group of CH in bond formation to form MR/CH nanoparticles. Fig. 5D depicts the presence of S atoms from sulfate groups of MR in the surface of nanoparticles with comparatively lesser density, which confirms the polyelectrolyte complexation of carboxylic and amino group leaving sulfate groups free to interact. Thus, we can propose the possibility of easy binding of sulfate group containing MR/CH particles to the cell receptors during drug delivery applications.

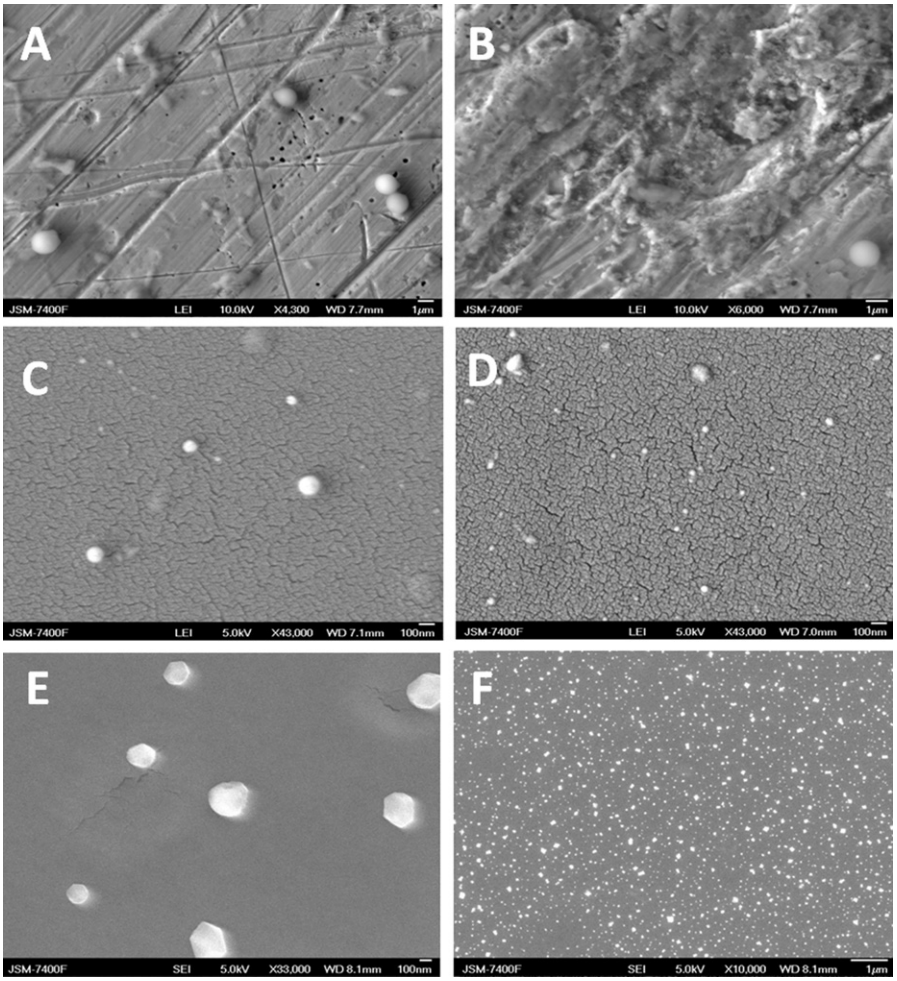

Fig. 3. SEM images of MR/CH nanoparticles on Sn substrate (A, B); SEM images of MR/CH nanoparticles on poly-L-lysine coated glass (C, D); SEM images of MR/CH nanoparticles on silica substrate (E, F).

Fig. 5E shows the Sn mapping profile of the Sn substrate used to attach MR/CH nanoparticles.

3.3. Drug encapsulation and release kinetics

Effective encapsulation of the drug, 5FU occurs while the polyelectrolyte complexation of MR and CH molecules during nanoparticle formulation. Fig. 6A shows the absorbance of drug loaded MR/CH nanoparticles and compared with free nanoparticles and 5FU. The peak intensity in the range of 260–300 nm shows the absorption of 5FU (Bakkialakshmi & Chandrakala, 2011). Amount of the drug loading can be determined by the analysis of supernatant for free drug using RP-HPLC and UV–vis spectrophotometer, after recovering the pellets holding the encapsulated drug, by ultracentrifugation. It was found that 1.03 ± 0.1 mg of drug was present in the supernatant after removing the pellet. This is approximately 40% of the total drug concentration, which shows that the 5FU loading achieved during nano-encapsulation is approximately 60% (w/w). However, when nanoparticles were subjected to a single wash, few of 5FU were dislodged to the medium, which is about 10% of the initial drug concentration. This indicates that almost 50% of the initial drug concentration was successfully encapsulated within the nanoparticles.

Drug release profile of 5FU encapsulated in the MR/CH nanoparticles was studied under a controlled condition of 37 °C with a uniform agitation of 100 rpm throughout the release kinetics experiment. Five different conditions were maintained with two different samples of 5FU loaded nanoparticles. Three months old set of sample stored under 4 °C was incubated at three different pH (4.5, 6.9 and 7.4) conditions and a freshly prepared sample were incubated at two different pH (6.9 and 7.4) conditions respectively. Fig. 6B shows the release of 5FU over a period of 12 days from washed MR/CH nanoparticles in aqueous phase. It was found that the release of the drug from MR/CH nanoparticles are relatively competent to other conventional drug delivery systems, where we can find an initial burst release within 24 h of time (Nair et al., 2011). It was evident from the studies that the amount of drug released within 24 h was below 5% and then it gradually raises during the consecutive days on incubation. Both old and new set of samples showed a different pattern of release at pH 7.4, though the stationary phases were acquired relatively at nearby time intervals. In case of the new set of sample under pH 7.4, drug release was in a slower pace till 6th day of incubation, later a sudden rise in release phase was observed, which is almost 40% of the cumulative drug concentration. This may be due to autocatalytic degradation of the particle matrix (Dunne, Corrigan, & Ramtoola, 2000). Comparatively, old set under the same conditions could only achieve a stationary phase after 10 days of incubation, which is around 23% of the drug encapsulated. This wide difference in release profile of 5FU between the new and old samples may be due to storage and the time dependent erosion of the drug from the later. In case of pH 6.9, new sample initially showed a slower ascent followed by a gradual increase of

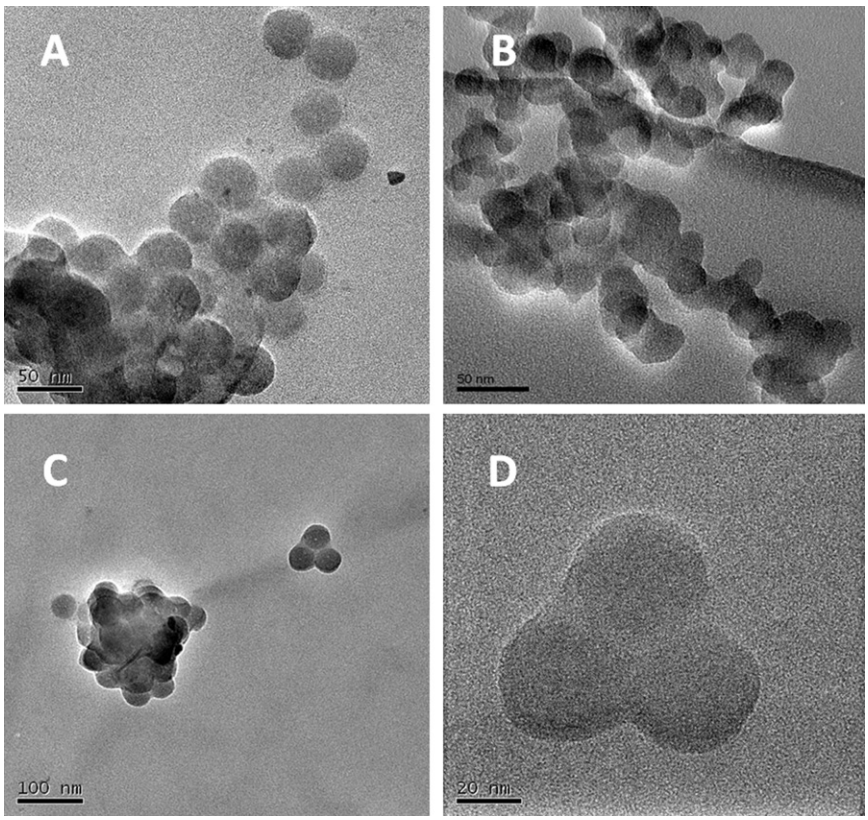

Fig. 4. TEM images showing the cluster morphology of MR/CH nanoparticles (A–D).

5FU concentration in the receptor phase after 4th day of incubation, where almost 50% of the drug was released at the end of the stationary phase. In contrast, old sample at pH 6.9 showed a steady rise after 3rd day of incubation until which it developed gradually and released around 55% of the encapsulated drug. It is evident from the drug kinetics curves that a cumulative maximum of 50% loaded drug can be released to the receptor phase under *in vitro* conditions irrespective of the sample nature, though old set at pH 7.4 shows a deviation of 28%. In case of acidic pH 4.5, a sustained and controlled pattern of release was observed till 9th day of incubation, which is

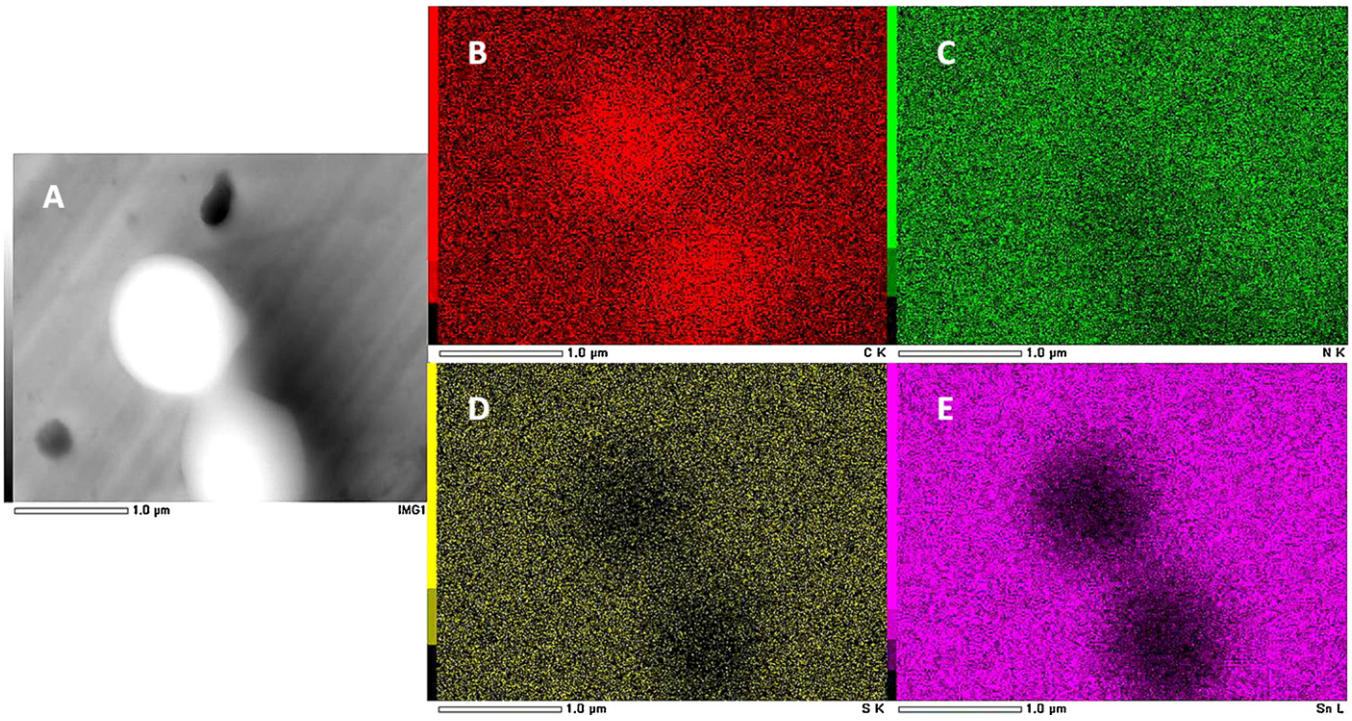

Fig. 5. SEM-EDS showing the elemental mapping of MR/CH nanoparticle. (A) EDS reference image; (B) carbon; (C) nitrogen; (D) sulfur; (E) tin.

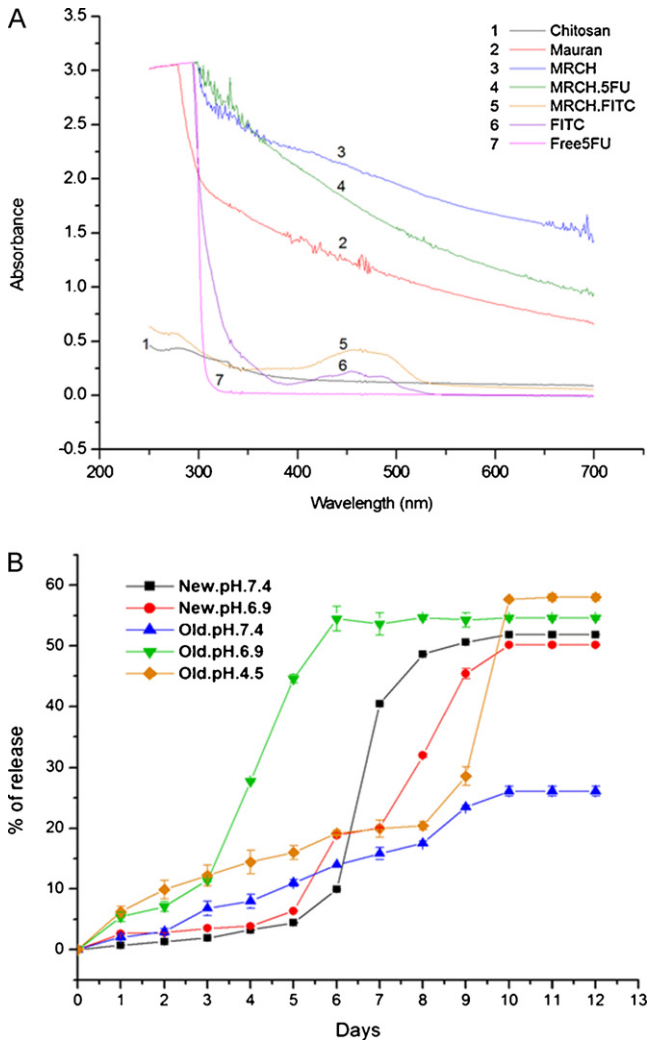

Fig. 6. (A) UV–vis absorption spectra; 1, CH; 2, MR; 3, MRCH; 4, MRCH-5FU; 5, MRCH-FITC; 6, FITC; 7, free-5FU; (B) 5FU release pattern from MR/CH nanoparticles at pH 4.5, 6.9 and pH 7.4.

~30% of the total concentration. Afterwards a sudden increase to 58% was observed leading to a stationary phase. Among the three different pH conditions tested, kinetics at acidic conditions enables a higher percentage of release, which can favor anticancer drug delivery using MR/CH nanoparticles. Also, we can assume that the release profiles attributed by 5FU loaded MR/CH nanoparticles are effective in any of the diseased conditions, where the pH of the blood plasma can either go acidic or alkaline beyond 7.45. Also it can be rendered *via* different routes of drug delivery where pH is an effective parameter for drug release. MR/CH nanoparticles displayed the evidence of sustained release of 5FU and hence can be ideal for controlled-release applications.

3.4. In vitro cytotoxicity and imaging

Biocompatibility of MR/CH nanoparticles was studied using normal mouse fibroblast cells, L929. Generally compounds which are cytotoxic in nature should drastically affect the growth of normal cells causing necrosis and cell death. Unlike algal polysaccharides, bacterial polysaccharides are believed to be immunogenic and toxic toward mammalian cells. But MR containing nanoparticles are proved to be biocompatible and non-cytotoxic in nature. Here, MR/CH nanoparticles treated L929 cells were found growing robust in the laboratory conditions without any observable cell damage. Fig. 7A shows the cytotoxic assay performed for L929 cells. It is clear from the graph that even the highest concentration of MR/CH nanoparticles showed 85% of cell viability though a minimal cytotoxicity of 15% was observed. Thus we can confirm that MR/CH nanoparticles are highly biocompatible and least cytotoxic in nature.

In vitro cytotoxicity of the 5FU-MR/CH nanoparticles in comparison with free 5FU was evaluated using MCF7, breast cancer cells. Fig. 7B and C shows the percentage of cell viability measured for free 5FU and 5FU-MR/CH nanoparticles respectively using alamar blue assay. Interestingly, on encapsulation of 5FU in to MR/CH nanoparticles a sustained release of drug ensuring a gradual killing of cancer cells was observed. In case of free drug, 83% of cells were found viable after 24 h whereas an abrupt decline in viability to 45% was observed after 48 h of incubation. Though as a thymidylate synthase inhibitor, free 5FU is good for killing cancer cells but at the same time it nonspecifically damages normal tissues leading to serious side effects (Nair et al., 2011). A maximum decrease in cell viability to ~11% was attained within 4th day of incubation with all three higher concentrations of free 5FU and after that there was no further killing observed. 5FU-MR/CH nanoparticles showed 73% of cell viability after 24 h compared to free 5FU (83% after 24 h) and later it declined gradually according to the sustained release of the drug from the MR/CH nanoparticles. The enhancement of cell death within 24 h treatment of 5FU-MR/CH nanoparticles to free 5FU may be due to the advantage of nanoparticulate mode of drug delivery. Since nanoscale particles are easy to internalize within the cells, increased drug retention within cells including solid tumors could be achieved by nanoparticulate drug delivery. More interestingly, the highest concentration of both 5FU-MR/CH nanoparticles and free 5FU is showing approximately same amount of decreased cell viability at the end of 5th day of incubation, which

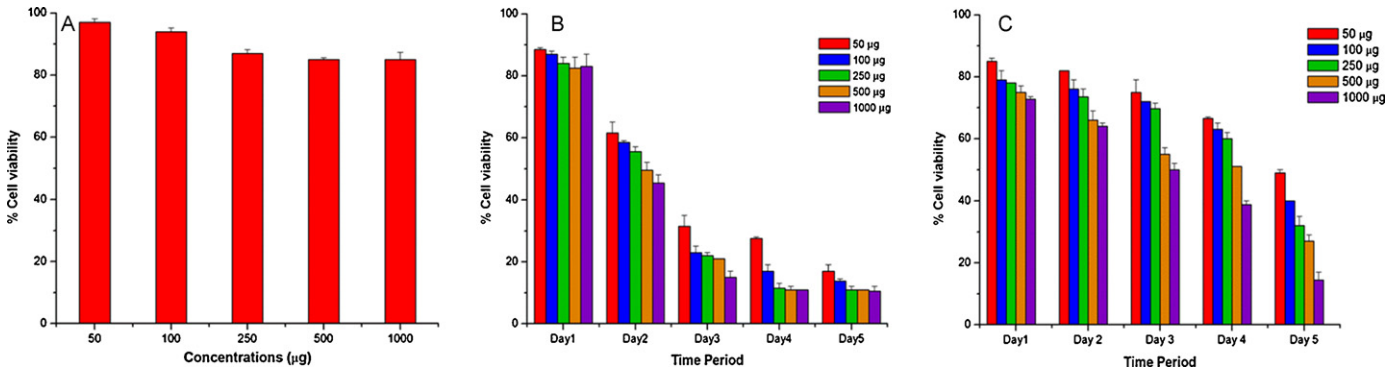

Fig. 7. Results of cytotoxicity assay: (A) MR/CH nanoparticles on L929 cells; (B) 5 days study of free 5FU on MCF7 cells; (C) 5 days study of 5FU loaded MR/CH nanoparticles on MCF7 cells.

is ~11 ± 3%. This implies the drug loaded MR/CH nanoparticles can competitively show an excellent anticancerous effect than free 5FU, without any side effects or normal tissue damage within its first five days of treatment. Similarly, cell uptake studies of MR/CH-FITC clearly show that fluorescent nanoparticles were bound and few were effectively localized within the cancer cells with respect to their varying sizes. Absorbance of MR/CH-FITC nanoparticles was compared with free MR/CH nanoparticles and FITC in Fig. 6A, which shows that the peak at 465 nm depicts the successful tagging of FITC. Fig. 8A shows the phase contrast image of MCF7 cells and Fig. 8B depicts the bright field image of MR/CH-FITC nanoparticle treated cells whereas Fig. 8C shows the epifluorescent image of the bound nanoparticles. Fig. 8D is the overlaid image of bright field and epifluorescent images.

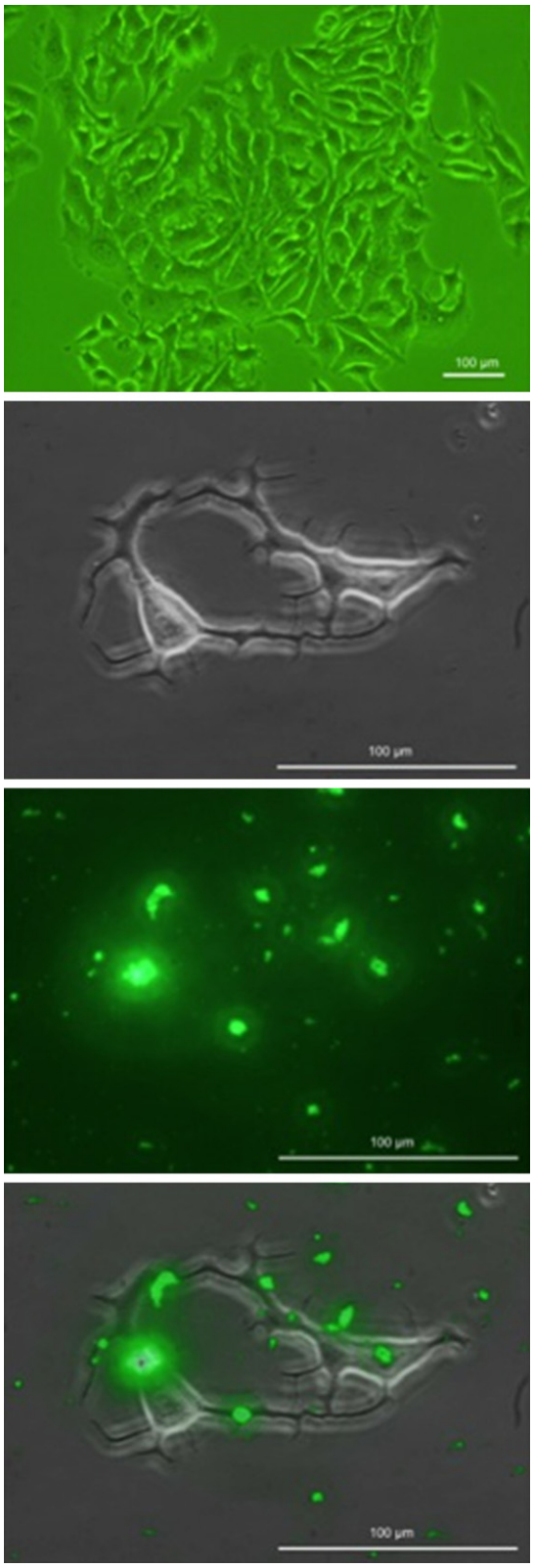

Fig. 8. (A) Phase contrast microscopic image of MCF7 cells; (B) bright field image; (C) epifluorescence image of MR/CH-FITC treated MCF7 cells; (D) merged image of B and C.

Generally SPS of eukaryotic origin was proved to be pharmaceutically ideal in treatment of various diseases whereas SPS of prokaryotic origin was considered antigenic, since they trigger immune mechanisms. Owing to the interesting properties of MR, it was challenging to apply them in the fields of nanotechnology and biomedicine. It is now proved from the *in vitro* assay using normal mouse fibroblast cells that MR is non-cytotoxic and biocompatible in nature. Hereby, we introduce a novel hybrid nanoparticle of MR and CH, which can be ideally applied for various biomedical applications as a bioactive drug delivery vehicle made of natural material. As a remedy for reducing repeated infusions of free drug and the side effects caused by its over dosages (Nair et al., 2011), we could employ the application of MR/CH nanoparticles as a targeted sustained drug delivery vehicle.

4. Conclusion

In summary, we have demonstrated the synthesis of an extremophilic bacterial sulfated polysaccharide based nanoparticles to address various applications in the field of bionanotechnology. It was found that the MR/CH nanoparticles are highly stable for at least 8 weeks in the solution and can be used for drug encapsulation and effective delivery under different pH conditions. Overall positive charge of the nanoparticles formed provides an insight of possible adsorption of negatively charged proteins or drugs for delivery purposes and its interaction as well as binding to the negatively charged sites of cell surfaces. Encapsulation of the hydrophilic drug, 5FU and its sustained delivery for a period of 10–12 days from MR/CH nanoparticles shows the possibility of its controlled release applications in therapeutic areas. This in turn will diminish the chances of risks causing due to continuous infusion of anticancer drugs. Similarly, the ability of MR/CH particles to withstand acidic and alkaline pH can favor different modes of drug delivery. Sustained and controlled release of 5FU to the dissolution medium under acidic pH favors its application in cancer chemotherapy. MR/CH nanoparticles can be successfully applied in chemotherapy to overcome the possible negative effects caused with overdosing of anticancer drugs and cytotoxic issues arising due to the polymer nanoparticles. Fluorescent dye tagged MR/CH nanoparticles showed an excellent mode of tracking system and cell imaging, which can be established more conveniently than other incompatible and insecure imaging techniques. The free sulfated groups present in the MR/CH nanoparticles could compete with host proteoglycan cell receptors in binding various antigenic determinants during disease mechanisms. Thus MR/CH nanoparticles widely open new frontiers for chemotherapy and biopharmaceutics. Furthermore, introduction of MR as a stable, biocompatible and biodegradable material with excellent properties is an alternative idea of exploring green nanotechnology.

Acknowledgements

Sreejith Raveendran and Aby C. Poulose would like to acknowledge their sincere gratitude to the Ministry of Education, Culture, Sports, Science and Technology (MEXT), Japan for the financial

support under the Monbukagakusho fellowship during the research. Also, part of this study has been supported by a grant for the programme of the strategic research foundation at private universities S1101017, organized by the MEXT, Japan since April 2012.

References

Arad, M. S., & Levy-Ontman, O. (2010). Red microalgal cell-wall polysaccharides: Biotechnological aspects. *Current Opinion in Biotechnology*, *21*, 358–364.

Argandona, M., Fernandez-Carazo, R., Llamas, I., Martinez-Checa, F., Caba, J. M., Quesada, E., et al. (2005). The moderately halophilic bacterium *Halomonas maura* is a free-living diazotroph. *FEMS Microbiology Letters*, *244*, 69–74.

Arias, S., Moral, A. D., Ferrer, M. R., Tallon, R., Quesada, E., & Bejar, V. (2003). Mauran, an exopolysaccharide produced by the halophilic bacterium *Halomonas maura*, with a novel composition and interesting properties for biotechnology. *Extremophiles*, *7*, 319–326.

Bakkialakshmi, S., & Chandrakala, D. (2011). A study on the interaction of 5-fluorouracil with human serum albumin using fluorescence quenching method. *Journal of Pharmaceutical Sciences and Research*, *3*, 1326–1329.

Bhumkar, R. D., & Pokharkar, B. V. (2006). Studies on effect of pH on cross-linking of CH with sodium tripolyphosphate: A technical note. *AAPS PharmaSciTech*, *7*. Article 50.

Bouchotroch, S., Quesada, E., Moral, A. D., Llamas, I., & Bejar, V. (2001). *Halomonas maura* sp. nov., a novel moderately halophilic, exopolysaccharide-producing bacterium. *International Journal of Systemic and Evolutionary Microbiology*, *51*, 1625–1632.

Calvo, C., Martinez-checa, F., Mota, A., Bejar, V., & Quesada, E. (1998). Effect of cations, pH and sulfate content on the viscosity and emulsifying activity of the *Halomonas eurihalina* exopolysaccharide. *Journal of Industrial Microbiology & Biotechnology*, *20*, 205–209.

Cheng, J., Huang, N., Lur, H., Kuo, C., & Lu, M. (2009). Characterization and biological functions of sulfated polysaccharides from sulfated-salt treatment of *Antrodia cinnamomea*. *Process Biochemistry*, *44*, 453–459.

Dev, A., Binulal, N. S., Anitha, A., Nair, S. V., Furuike, T., Tamura, H., et al. (2010). Preparation of poly(lactic acid)/CH nanoparticles for anti-HIV drug delivery applications. *Carbohydrate Polymers*, *80*, 833–838.

Dubois, M., Gilles, K. A., Hamilton, J. K., Rebers, P. A., & Smith, F. (1956). Colorimetric method for determination of sugars and related substances. *Analytical Chemistry*, *28*(3), 350–356.

Dunne, M., Corrigan, O. I., & Ramtoola, Z. (2000). Influence of particle size and dissolution conditions on the degradation properties of polylactide-co-glycolide particles. *Biomaterials*, *21*, 1659–1668.

Ge, Y., Zhang, Y., He, S., Nie, F., Teng, G., & Gu, N. (2006). Fluorescence modified CH-coated magnetic nanoparticles for high-efficient cellular imaging. *Nanoscale Research Letters*, *4*, 287–295.

Gomez-Ordonez, E., & Ruperez, P. (2011). FTIR-ATR spectroscopy as a tool for polysaccharide identification in edible brown and red seaweeds. *Food Hydrocolloids*, *25*, 1514–1520.

Grenha, A., Gomes, M. E., Rodrigues, M., Santo, V. E., Mano, J. F., Neves, N. M., et al. (2010). Development of new CH/carrageenan nanoparticles for drug delivery applications. *Journal of Biomedical Materials Research Part A*, *92*, 1265–1272.

Hosoyo, M., Balzarini, J., Shigeta, S., & Clercq, E. D. (1991). Differential inhibitory effects of sulfated polysaccharides and polymers on the replication of various myxoviruses and retroviruses, depending on the composition of the target amino acid sequences of the viral envelope glycoproteins. *Antimicrobial Agents and Chemotherapy*, *35*, 2515–2520.

Huang, L., Sui, W., Wang, Y., & Jiao, Q. (2010). Preparation of CH/chondroitin sulfate complex microcapsules and application in controlled release of 5-fluorouracil. *Carbohydrate Polymers*, *80*, 168–173.

Janes, K. A., Calvo, P., & Alonso, M. J. (2001). Polysaccharide colloidal particles as delivery systems for macromolecules. *Advanced Drug Delivery Reviews*, *47*, 83–97.

Lin, Y., Chang, C., Wu, Y., Hsu, Y., Chiou, S., & Chen, Y. (2009). Development of pH-responsive CH/heparin nanoparticles for stomach-specific anti-*Helicobacter pylori* therapy. *Biomaterials*, *30*, 3332–3342.

Liu, Z., Jiao, Y., Liu, F., & Zhang, Z. (2007). Heparin/CH nanoparticle carriers prepared by polyelectrolyte complexation. *Journal of Biomedical Materials Research Part A*, *83*, 806–812.

Liu, Z., Jiao, Y., Wang, Y., Zhou, C., & Zhang, Z. (2008). Polysaccharides-based nanoparticles as drug delivery systems. *Advanced Drug Delivery Reviews*, *60*, 1650–1662.

Llamas, I., Moral, A. D., Martinez-Checa, F., Arco, Y., Arias, S., & Quesada, E. (2006). *Halomonas maura* is a physiologically versatile bacterium of both ecological and biotechnological interest. *Antonie van Leeuwenhoek*, *89*, 395–403.

Luscher-Mattil, M. (2000). Polyanions—A lost chance in the fight against HIV and other virus diseases? *Antiviral Chemistry & Chemotherapy*, *11*, 249–259.

McCarron, P. A., Woolfson, A. D., & Keating, S. M. (2000). Sustained release of 5-fluorouracil from polymeric nanoparticles. *Journal of Pharmacy and Pharmacology*, *52*(12), 1451–1459.

Nair, L. K., Jagadeeshan, S., Nair, S. A., & Kumar, G. S. V. (2011). Biological evaluation of 5-fluorouracil nanoparticles for cancer chemotherapy and its dependence on the carrier, PLGA. *International Journal of Nanomedicine*, *6*, 1685–1697.

Nicholas, C. M., Lardiere, S. G., Bowman, J. P., Nichols, P. D., Gibson, J. A. E., & Guezennec, J. (2005). Chemical characterization of exopolysaccharides from Antarctic marine bacteria. *Microbial Ecology*, *49*, 578–589.

Quesada, E., Valderrama, M. J., Bejar, V., Ventosa, A., Gutierrez, M. C., Ruiz-Berraquero, F., et al. (1990). *Volcaniella eurihalina* gene nov sp. nov. a moderately halophilic nonmotile gram-negative rod. *International Journal of Systemic Bacteriology*, 261–267.

Rougeaux, H., Pichon, R., Kervarec, N., Raguenes, G. H. C., & Guezennec, J. G. (1996). Novel bacterial exopolysaccharides from deep sea hydrothermal vents. *Carbohydrate Polymers*, *31*, 237–242.

Santo, V. E., Duarte, A. R. C., Gomes, M. E., Mano, J. F., & Reis, R. L. (2010). Hybrid 3D structure of poly(D,L-lactic acid) loaded with CH/chondroitin sulfate nanoparticles to be used as carriers for biomacromolecules in tissue engineering. *Journal of Supercritical Fluids*, *54*, 320–327.

Sivabalan, M., Shering, A., Reddy, P., Vasudevaiah, Jose, A., & Nigila, G. (2011). Formulation and evaluation of 5-fluorouracil loaded CH and eudragit nanoparticles for cancer therapy. *Pharmacie Globale (IJCP)*, *2*, 1–4.

Smith, P. K., Krohn, R. I., Hermanson, G. T., Mallia, A. K., Gartner, F. H., Provenzano, M. D., et al. (1985). Measurement of protein using bicinchoninic acid. *Analytical Biochemistry*, *150*(1), 76–85.

Toshihiko, T., Amornrut, C., & Robert, J. L. (2003). Structure and bioactivity of sulfated polysaccharides. *Trends in Glycoscience and Glycotechnology*, *15*(81), 29–46.

Xu, T., Zhang, N., Nichols, H. L., Shi, D., & Wen, X. (2007). Modification of nanostructured materials for biomedical applications. *Material Science & Engineering C*, *27*, 579–594.